QUARTERLY OF APPLIED MATHEMATICS
VOLUME LIII, NUMBER 2
JUNE 1995, PAGES 353–381

THE MODELING OF PIEZOCERAMIC PATCH INTERACTIONS WITH SHELLS, PLATES, AND BEAMS

BY

H. T. BANKS (*North Carolina State University, Raleigh, North Carolina*)

R. C. SMITH (*NASA Langley Research Center, Hampton, Virginia*)

AND

YUN WANG (*North Carolina State University, Raleigh, North Carolina*)

Abstract. General models describing the interactions between one or a pair of piezoceramic patches and elastic substructures consisting of a cylindrical shell, plate, or beam are presented. In each case, the contributions to the internal moments and forces due to the presence of the patches are carefully discussed. In addition to these material contributions, the input of voltage to the patches produces mechanical strains that lead to external moments and forces. These external loads depend on the material properties of the patch, the geometry of patch placement, and the voltage. The internal and external moments and forces due to the patches are then incorporated into the equations of motion, which yields models describing the dynamics of the combined structure. These models are sufficiently general to allow for potentially different patch voltages, which implies that they can be suitably employed when using piezoceramic patches for controlling system dynamics when both extensional and bending vibrations are present.

1. Introduction. The use of piezoceramic elements as sensors and actuators has burgeoned in the last several years in applications ranging from the measurement and damping of vibrations in large flexible structures to the control of noise in structural acoustics settings. Their utility as sensors derives from the property that when the element is subjected to a mechanical strain, a voltage proportional to the strain is produced. Conversely, they also exhibit the phenomenon that an applied polarization voltage across the unconstrained element produces in-plane mechanical strains in the

Received December 9, 1992.
1991 *Mathematics Subject Classification.* Primary 35Q72, 35R05, 73K12.
The research of H. T. B. and Y. W. was supported in part by the Air Force Office of Scientific Research under grant AFOSR-90-0091. This research was also supported by the National Aeronautics and Space Administration under NASA Contract Numbers NAS1-18605 and NAS1-19480 while H. T. B. was a visiting scientist and R. C. S. was in residence at the Institute for Computer Applications in Science and Engineering (ICASE), NASA Langley Research Center, Hampton, VA 23681. Finally, the work of H. T. B. was completed in part while the author was a visitor at the Institute for Mathematics and Its Applications, University of Minnesota, Minneapolis, MN 55455.

material. Because of these properties, piezoceramic elements have found increasing success both as sensors such as strain gauges and accelerometers and as distributed actuators. Their success as actuators is augmented by the fact that they can be used to directly control local vibrations without applying rigid body forces and torques, and, due to their distributed nature, they are less prone to spillover effects in many control strategies. Moreover, the piezoceramic elements or patches are inexpensive, lightweight, space efficient, and can be easily shaped or bonded to a variety of surfaces. Hence a large number of patches can be used to sense and control without significantly changing the mass or dynamic properties of the system.

In order to obtain optimal results with the piezoceramic elements or patches in sensing and control applications, it is necessary to have accurate models of the mechanics of induced strain actuation. This modeling also provides knowledge of the physical limitations of the piezoceramic patches as actuators in various settings. Detailed models have been developed for piezoceramic patch interaction with Euler-Bernoulli beams [2, 3, 4, 5, 10] and thin plates [6, 13]. Because many of the initial applications of piezoceramic elements were in settings involving the sensing and control of bending deformations (these vibrations are dominant in many low-frequency vibration and noise-control problems), most of these models concentrate on patch configurations that excite pure bending motion of the substructure with more limited discussions of pure extensional excitation. It was not until [10] that a model was developed that provided for simultaneous excitation of both bending and extensional deformations in an Euler-Bernoulli beam. One motivation for developing such a model is the observation that in complex coupled systems, in-plane vibrations with small displacements can have large in-plane energy levels due to the property that beams are much stiffer in extension than in bending. This in-plane energy can then couple into flexural vibrations at structural discontinuities such as joints, thus necessitating the control of both bending and extensional vibrations in such structures. As determined by Fuller et al [8] through experimental work, simultaneous reductions in bloth flexural and extensional deformations in a beam can be obtained through the use of asymmetric pairs of piezoceramic actuators and sensors in adaptive control schemes, and the analytic work in [10] was a first step toward developing a model that could be used in further such control settings. In that work, force and moment balancing were used to determine expressions for the moments and strains induced by the activation of a single piezoceramic patch that was bonded to an Euler-Bernoulli beam.

In addition to beams and plates, thin elastic shells are often used to describe various structural components as well as for modeling the coupling between structural vibrations and their radiating or receiving acoustic fields. For example, the transmission of sound through an airplane fuselage due to low-frequency, high-amplitude exterior acoustic fields can be modeled by a vibrating thin cylindrical shell that is coupled to an interior acoustic pressure field [9]. In order to optimally control the interior noise via piezoceramic patch actuation, one first needs to model accurately the interactions between the patches and the shell. This raises modeling issues that differ from those encountered in the beam and plate analyses in that the in-plane and

bending vibrations are coupled in the cylindrical shell due to curvature effects.

Analytical models describing piezoceramic patch/cylindrical shell interactions have primarily been based on layered-shell theory [12, 23] or the use of flat plate piezoceramic coupling results when determining the resulting loading on the shell [17]. In the first case it is assumed that the piezoceramic material makes up an entire layer of the elastic structure, and so this model is of limited use when considering small patches as actuators. When using the flat plate theory, it is assumed that the patch dimensions are small in comparison with the cylinder radius. Curvature properties are then neglected when modeling the coupling between the patch and shell and determining the loading due to activation of the patch.

In this work, we present general models describing the dynamics of structures comprised of piezoceramic patches that are bonded to elastic substructures consisting of a beam, plate, or thin cylindrical shell. These results differ from those obtained previously both in their generality (curvature effects are retained in the shell interactions, differing patch voltages are allowed, etc.) and in the care taken to differentiate between and separate the internal (material) and external moments and forces that are generated by the patches. Specifically, when the piezoceramic patches are bonded to the substructure, the basic equations are affected in two ways. The first is due to the fact that the presence of the patches on the beam, plate, or shell changes the material properties of the structure since the patches add thickness and have Young's moduli, damping coefficients, and Poisson ratios which in general differ from those of the underlying substructure. These differences in material characteristics lead to additional terms in the internal moment and force resultants which, as illustrated in [1], must be accounted for in order to match system frequencies when estimating physical parameters. The second contribution due to the piezoceramic patches results from the strains that are induced by an applied voltage. This leads to the generation of external moments and forces that enter the equations of motion as external loads.

The inclusion of these internal and external moment and force expressions into the equations of motion leads to models that consistently describe both the passive and active contributions due to the patches. These models are sufficiently general so as to allow for differing voltages into the patches (including the possibility of an inactive patch receiving no voltage). From a control perspective, these models are important since they provide for greater latitude in designing control strategies involving the use of piezoceramic elements to affect both the bending and extensional properties of a structure.

As a prelude to the development of the patch interaction models, equations of motion for the underlying substructures are presented, with special attention paid to the contributions due to externally applied moments and forces since this is where the interactions between the patches and substructure occur. The analysis leading up to the structural equations also motivates many of the techniques that are used to develop the patch interaction models.

To this end, a synopsis of the derivation of the strong form of the time-dependent Donnell-Mushtari thin-shell equations from Newtonian principles (force and moment balancing) is presented in Sec. 2. A complete treatment of this topic can be

found in [14, 16, 19, 21, 22], and so our discussion is limited to summarizing that material that is needed for developing the shell/patch interaction model as presented in Sec. 3. The choice of the Donnell-Mushtari model is for ease of presentation, and, as noted at various points in the discussion, the patch/shell interaction model can be easily extended to higher-order models as warranted by the physical situation.

An inherent disadvantage of the strong form for the equilibrium equations when the external loads are generated by piezoceramic elements is the resulting presence of the first and second derivatives of the Heaviside function due to the finite support of the patches. As a result of this as well as other parameter estimation and approximation issues, we then develop the weak form of the time-dependent Donnell-Mushtari shell equations. This is done in more detail, since this development is less readily available in the literature. This formulation is advantageous in many approximation schemes, admits the estimation of discontinuous material parameters, and eliminates the problem of differentiating the Heaviside function since the derivatives are transferred onto the test functions.

Section 2 concludes with a synopsis of the strong and weak forms of the Kirchhoff plate and Euler-Bernoulli beam equations. As in the shell discussion, particular emphasis is placed on the contributions of externally applied forces and moments, since this is where the coupling between the substructure and piezoceramic patches occurs.

The patch contributions to the cylindrical shell equations are developed in Sec. 3. As mentioned previously, these contributions consist of internal (material) and external moments and forces. The internal moments and forces account for the material changes in the structure due to the presence of the patches and are present even when no voltage is being applied to the patches. The external contributions are due to the strains induced by the patches when voltage is applied, and they enter the equations of motion as external loads.

In Sec. 4, the techniques of Sec. 3 are tailored to composite structures consisting of piezoceramic patches that are bonded to plates and beams. Due to their generality, the models allow for complex interactions involving both bending and extensional components, since the voltages and material properties of the individual patches can differ (e.g., the mere presence of a single patch on a beam leads to coupling between the partial differential equations (PDEs) describing transverse and longitudinal motion, since the structure is no longer symmetric). As with the shells, this provides structure/patch interaction models that can be used in various structural and structural acoustics control settings.

2. Underlying shell, plate, and beam equations. Throughout this discussion, we consider a thin circular cylindrical shell of radius R, thickness h, and having the axial coordinate x as shown in Figure 1. The variable z measures the distance of a point on the shell from the corresponding point on the middle surface ($z = 0$) along the normal to the middle surface.

Strain-displacement relations. By combining Love's shell assumptions with the strain-displacement equations of three-dimensional elasticity theory, one obtains the

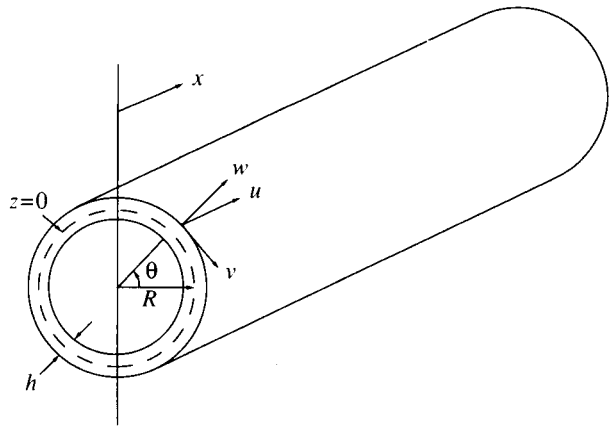

FIG. 1. The cylindrical thin shell

strain relations

$$\begin{aligned} e_x &= \varepsilon_x + z\kappa_x, \\ e_\theta &= \frac{1}{1 + \underline{z/R}}(\varepsilon_\theta + z\kappa_\theta), \\ \gamma_{x\theta} &= \frac{1}{1 + \underline{z/R}}\left[\varepsilon_{x\theta} + z\left(1 + \frac{z}{2R}\right)\tau\right], \end{aligned} \tag{2.1}$$

where e_x and e_θ are normal strains at an arbitrary point within the cylindrical shell and $\gamma_{x\theta}$ is the shear strain. Here ε_x, ε_θ, and $\varepsilon_{x\theta}$ are the normal and shear strains in the middle surface, and κ_x, κ_θ, and τ are the midsurface changes in curvature and midsurface twist (see [16], p. 8).

Note that within the framework of infinitesimal elasticity, the equations (2.1) are exact and in the Byrne-Flügge-Lur'ye shell theory, these represent the exact form of the kinematic equations. In the Donnell-Mushtari theory, one neglects the underlined terms z/R with respect to unity, thus leaving

$$\begin{aligned} e_x &= \varepsilon_x + z\kappa_x, \\ e_\theta &= \varepsilon_\theta + z\kappa_\theta, \\ \gamma_{x\theta} &= \varepsilon_{x\theta} + z\left(1 + \frac{z}{2R}\right)\tau. \end{aligned} \tag{2.2}$$

In terms of the axial, tangential, and radial displacements u, v, and w, respectively, the expressions for the midsurface strains and changes in curvature for the cylindrical shell are

$$\begin{aligned} \varepsilon_x &= \frac{\partial u}{\partial x}, & \kappa_x &= -\frac{\partial^2 w}{\partial x^2} \\ \varepsilon_\theta &= \frac{1}{R}\frac{\partial v}{\partial \theta} + \frac{w}{R}, & \kappa_\theta &= -\frac{1}{R^2}\frac{\partial^2 w}{\partial \theta^2} + \frac{1}{\underline{R^2}}\frac{\partial v}{\partial \theta} \\ \varepsilon_{x\theta} &= \frac{\partial v}{\partial x} + \frac{1}{R}\frac{\partial u}{\partial \theta}, & \tau &= -\frac{2}{R}\frac{\partial^2 w}{\partial x \partial \theta} + \frac{2}{\underline{R}}\frac{\partial v}{\partial x}. \end{aligned} \tag{2.3}$$

As before, the underlined terms are retained in the Byrne, Flügge, and Lur'ye theory and are discarded in the Donnell-Mushtari theory. We point out that the equations (2.1) and (2.3) differ from those arising in the theory of flat plates both in the presence of the length differential $Rd\theta$ as well as in the retention of the strain terms ε_x and ε_θ (only bending contributions are considered in the corresponding models of the transverse vibrations of a flat plate).

Stress-strain relations. To determine the constitutive properties of the shell, it is assumed that the shell material is elastic and isotropic. Hooke's law in conjunction with the assumption that the transverse shear stresses σ_{xz} and $\sigma_{\theta z}$ as well as the normal strain component e_z are small in comparison with other stresses and strains (these conditions are part of Love's third and fourth assumptions) then yields

$$\begin{aligned} \sigma_x &= \frac{E}{1-\nu^2}(e_x + \nu e_\theta), \\ \sigma_\theta &= \frac{E}{1-\nu^2}(e_\theta + \nu e_x), \\ \sigma_{x\theta} = \sigma_{\theta x} &= \frac{E}{2(1+\nu)}\gamma_{x\theta}, \end{aligned} \tag{2.4}$$

where σ_x and σ_θ are normal stresses and $\sigma_{x\theta}$ and $\sigma_{\theta x}$ are tangential shear stresses. The constants E and ν are the Young's modulus and Poisson ratio for the shell.

Force and moment resultants. By integrating the stresses over the face of a fundamental element, the force resultants can be expressed as

$$\begin{bmatrix} N_x \\ N_{x\theta} \\ Q_x \end{bmatrix} = \int_{-h/2}^{h/2} \begin{bmatrix} \sigma_x \\ \sigma_{x\theta} \\ \sigma_{xz} \end{bmatrix} \left(1 + \frac{z}{\underline{R}}\right) dz \tag{2.5}$$

and

$$\begin{bmatrix} N_\theta \\ N_{\theta x} \\ Q_\theta \end{bmatrix} = \int_{-h/2}^{h/2} \begin{bmatrix} \sigma_\theta \\ \sigma_{\theta x} \\ \sigma_{\theta z} \end{bmatrix} dz. \tag{2.6}$$

Similarly, the moment resultants are

$$\begin{bmatrix} M_x \\ M_{x\theta} \end{bmatrix} = \int_{-h/2}^{h/2} \begin{bmatrix} \sigma_x \\ \sigma_{x\theta} \end{bmatrix} \left(1 + \frac{z}{\underline{R}}\right) z\, dz \tag{2.7}$$

and

$$\begin{bmatrix} M_\theta \\ M_{\theta x} \end{bmatrix} = \int_{-h/2}^{h/2} \begin{bmatrix} \sigma_\theta \\ \sigma_{\theta x} \end{bmatrix} z\, dz. \tag{2.8}$$

The orientations of the various forces and moments are shown in Fig. 2. We point out that the transverse shear stresses σ_{xz} and $\sigma_{\theta z}$ are used when obtaining the force resultants Q_x and Q_θ even though they are omitted in the constitutive relations. This is one of the contradictions that arises in the classical shell theory.

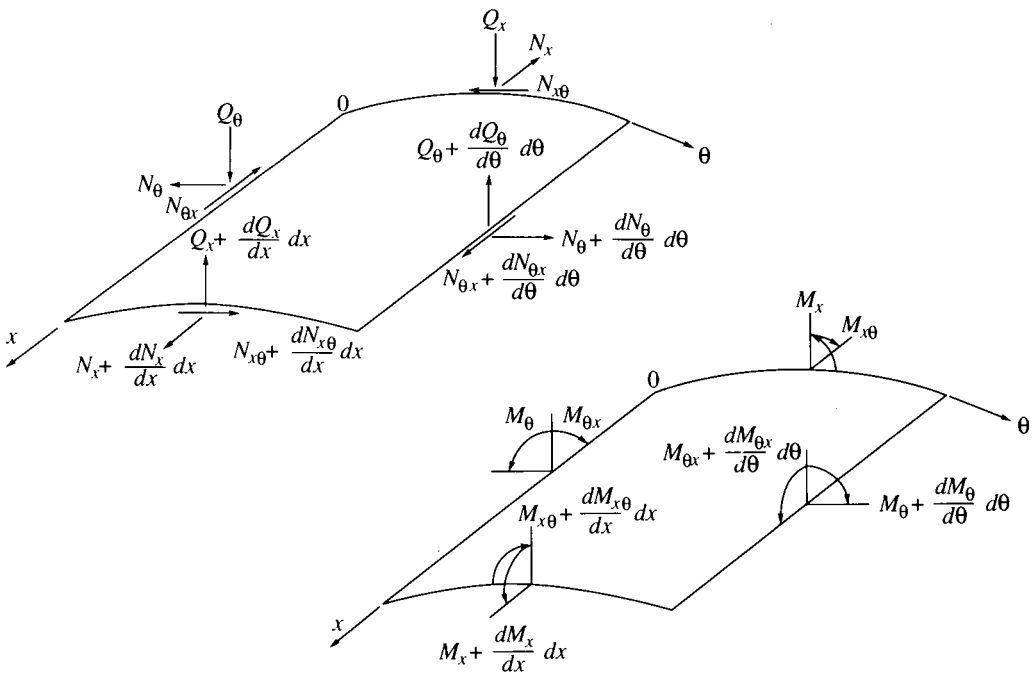

FIG. 2. Force and moment resultants for the cylindrical shell

In the Donnell-Mushtari theory the underlined terms z/R are neglected in comparison to unity, and the integrals are determined accordingly, to yield

$$
\begin{aligned}
N_x &= \frac{Eh}{(1-\nu^2)}\left[\frac{\partial u}{\partial x} + \nu\left(\frac{1}{R}\frac{\partial v}{\partial \theta} + \frac{w}{R}\right)\right], \\
M_x &= -\frac{Eh^3}{12(1-\nu^2)}\left[\frac{\partial^2 w}{\partial x^2} + \frac{\nu}{R^2}\frac{\partial^2 w}{\partial \theta^2}\right], \\
N_\theta &= \frac{Eh}{(1-\nu^2)}\left[\frac{1}{R}\frac{\partial v}{\partial \theta} + \frac{w}{R} + \nu\frac{\partial u}{\partial x}\right], \\
M_\theta &= -\frac{Eh^3}{12(1-\nu^2)}\left[\frac{1}{R^2}\frac{\partial^2 w}{\partial \theta^2} + \nu\frac{\partial^2 w}{\partial x^2}\right], \\
N_{x\theta} &= N_{\theta x} = \frac{Eh}{2(1+\nu)}\left[\frac{\partial v}{\partial x} + \frac{1}{R}\frac{\partial u}{\partial \theta}\right], \\
M_{x\theta} &= M_{\theta x} = -\frac{Eh^3}{12R(1+\nu)}\frac{\partial^2 w}{\partial x \partial \theta}.
\end{aligned}
\tag{2.9}
$$

Similar expressions are obtained in the higher-order theories.

Strong form of the Donnell-Mushtari shell equations. The equations of the dynamic equilibrium of the element are obtained by balancing the internal force and moment resultants as shown in Fig. 2 with any externally applied forces and moments. Let

$$\vec{q} = \hat{q}_x \hat{i}_x + \hat{q}_\theta \hat{i}_\theta + \hat{q}_n \hat{i}_n$$

and

$$\vec{m} = \hat{m}_x \hat{i}_x + \hat{m}_\theta \hat{i}_\theta$$

denote the surface forces and moments due to an external field that is acting on the middle surface. Hence $\vec{q}$ and $\vec{m}$ have units of force and moment per unit area, respectively.

Considering equilibrium of the forces in the x, θ, and z directions yields

$$\begin{aligned} R\frac{\partial N_x}{\partial x} + \frac{\partial N_{\theta x}}{\partial \theta} + R\hat{q}_x &= 0, \\ \frac{\partial N_\theta}{\partial \theta} + R\frac{N_{x\theta}}{\partial x} + Q_\theta + R\hat{q}_\theta &= 0, \\ R\frac{\partial Q_x}{\partial x} + \frac{\partial Q_\theta}{\partial \theta} - N_\theta + R\hat{q}_n &= 0, \end{aligned} \tag{2.10}$$

respectively. In the Donnell-Mushtari theory, the transverse shearing force Q_θ is considered to be negligible in the second equation of (2.10) and is subsequently neglected when determining the final equilibrium equations. Similarly, with 0 as a reference origin, the balancing of moments with respect to θ, x, and z yields

$$\begin{aligned} R\frac{\partial M_x}{\partial x} + \frac{\partial M_{\theta x}}{\partial \theta} - RQ_x + R\hat{m}_\theta &= 0, \\ \frac{\partial M_\theta}{\partial \theta} + R\frac{\partial M_{x\theta}}{\partial x} - RQ_\theta + R\hat{m}_x &= 0, \\ N_{x\theta} - N_{\theta x} - \frac{M_{\theta x}}{R} &= 0, \end{aligned} \tag{2.11}$$

respectively. By referring to the integral definitions of $N_{x\theta}$, $N_{\theta x}$, and $M_{\theta x}$, it can be seen that the third expression in (2.11) is identically satisfied due to the symmetry of the stress tensor.

Time enters the equilibrium equations through the inertial terms; hence for time-dependent problems the force $\hat{q}_x$ is replaced by

$$-\rho h\frac{\partial^2 u}{\partial t^2} + \hat{q}_x,$$

where ρ is the density in mass per unit volume of the shell. Similar substitutions are made for $\hat{q}_\theta$ and $\hat{q}_n$. By combining (2.10) and (2.11), one arrives at the time-dependent Donnell-Mushtari equilibrium equations for a thin cylindrical shell with radius of curvature R and thickness h:

$$\begin{aligned} R\rho h\frac{\partial^2 u}{\partial t^2} - R\frac{\partial N_x}{\partial x} - \frac{\partial N_{\theta x}}{\partial \theta} &= R\hat{q}_x, \\ R\rho h\frac{\partial^2 v}{\partial t^2} - \frac{\partial N_\theta}{\partial \theta} - R\frac{N_{x\theta}}{\partial x} &= R\hat{q}_\theta, \\ R\rho h\frac{\partial^2 w}{\partial t^2} - R\frac{\partial^2 M_x}{\partial x^2} - \frac{1}{R}\frac{\partial^2 M_\theta}{\partial \theta^2} - 2\frac{\partial^2 M_{x\theta}}{\partial x \partial \theta} + N_\theta &= R\hat{q}_n + R\frac{\partial \hat{m}_\theta}{\partial x} + \frac{\partial \hat{m}_x}{\partial \theta}. \end{aligned} \tag{2.12}$$

We note that the representation of the external loads as surface moments and forces is convenient when deriving the strong form of the equations of motion. However, in many applications where it is necessary to actually determine expressions for these loads or when using the weak form of the equations, it is advantageous

to represent these loads in terms of line forces and moments. To accomplish this, let $\hat{M}_x$, $\hat{M}_\theta$, $\hat{N}_x$, and $\hat{N}_\theta$ denote the external resultants acting on the edge of an infinitesimal element which have the same orientation as the internal resultants depicted in Fig. 2 (with units of moment and force per unit length of middle surface). Force and moment balancing can be used to write the area moments and in-plane forces in terms of these line moments and forces, thus yielding

$$\hat{q}_x = -\frac{\partial \hat{N}_x}{\partial x}, \quad \hat{q}_\theta = -\frac{1}{R}\frac{\partial \hat{N}_\theta}{\partial \theta}, \quad \hat{m}_x = -\frac{1}{R}\frac{\partial \hat{M}_\theta}{\partial \theta}, \quad \hat{m}_\theta = -\frac{\partial \hat{M}_x}{\partial x}. \tag{2.13}$$

We point out that the first expression in (2.13) can be obtained from (2.10) simply by replacing N_x by $\hat{N}_x$ and deleting $\partial N_{\theta x}/\partial \theta$ in the first expression of (2.10). Similar analysis leads to the other expressions in (2.13). The use of these line moments and forces in (2.12) is equivalent to including the external resultants directly when determining the equations of moment and force equilibrium for an infinitesimal shell element as done in (2.10) and (2.11).

The substitution of the internal moments and forces in (2.9) and the external resultants from (2.13) then yields

$$\begin{aligned}
&\frac{1}{C_L^2}\frac{\partial^2 u}{\partial t^2} - \frac{\partial^2 u}{\partial x^2} - \frac{1-\nu}{2R^2}\frac{\partial^2 u}{\partial \theta^2} - \frac{1+\nu}{2R}\frac{\partial^2 v}{\partial x \partial \theta} - \frac{\nu}{R}\frac{\partial w}{\partial x} \\
&\qquad = -\frac{(1-\nu^2)}{Eh}\frac{\partial \hat{N}_x}{\partial x}, \\
&\frac{1}{C_L^2}\frac{\partial^2 v}{\partial t^2} - \frac{1-\nu}{2}\frac{\partial^2 v}{\partial x^2} - \frac{1}{R^2}\frac{\partial^2 v}{\partial \theta^2} - \frac{1+\nu}{2R}\frac{\partial^2 u}{\partial x \partial \theta} - \frac{1}{R^2}\frac{\partial w}{\partial \theta} \\
&\qquad = -\frac{(1-\nu^2)}{Eh}\frac{1}{R}\frac{\partial \hat{N}_\theta}{\partial \theta}, \\
&\frac{1}{C_L^2}\frac{\partial^2 w}{\partial t^2} + \frac{\nu}{R}\frac{\partial u}{\partial x} + \frac{1}{R^2}\frac{\partial v}{\partial \theta} + \frac{1}{R^2}w + \frac{h^2}{12}\nabla^4 w \\
&\qquad = \frac{(1-\nu^2)}{Eh}\left[\hat{q}_n - \frac{1}{R^2}\frac{\partial^2 \hat{M}_\theta}{\partial \theta^2} - \frac{\partial^2 \hat{M}_x}{\partial x^2}\right],
\end{aligned} \tag{2.14}$$

where again, u, v, and w are the axial, tangential, and radial displacements, respectively [16]. The constant C_L given by

$$C_L = \left[\frac{E}{\rho(1-\nu^2)}\right]^{1/2}$$

is the phase speed of axial waves in the cylinder wall. The external line forces $\hat{N}_x$ and $\hat{N}_\theta$ and moments $\hat{M}_x$ and $\hat{M}_\theta$ have units of force and moment per unit length of the middle surface, respectively, and are generated in our problem by the activation of the piezoceramic patches. The load $\hat{q}_n$ is left as a surface force, since this is the form that it usually takes in problems involving the excitation of a shell through normal forces (an example of a normal force in this form is the pressure exerted on the shell due to an exterior or interior acoustic field).

We again emphasize that the resultant expressions in (2.13) (and hence the system (2.14)) were derived for an infinitesimal element; hence certain modifications must be made when considering the *global* form of the resultants and equations (as is necessary when the resultants are generated by a piezoceramic patch). In certain cases (e.g., for certain types of moments and forces), the system (2.14) agrees with the strong form of the global shell equations. In general, however, this is not true, and one must exercise extreme care in determining the form of the global representations for the moments and forces.

Weak form of the Donnell-Mushtari cylindrical shell equations. In order to find the weak form of the shell equations, the kinetic and strain energies of the shell are needed. By combining the Kirchhoff shell hypothesis with the strain results from classical elasticity theory, it follows that the strain energy stored in the shell during deformation is given by

$$U = \frac{1}{2}\int_{-h/2}^{h/2}\int_0^{2\pi}\int_0^{l}(\sigma_x e_x + \sigma_\theta e_\theta + \sigma_{x\theta}\gamma_{x\theta})(1 + z/R)R\,dx\,d\theta\,dz\,,$$

where the strains and stresses are given in (2.1) and (2.4), respectively. Substitution and integration (with $(1 + z/R)^{-1}$ replaced by its geometric series expansion and neglecting powers of z in the integrand which are greater than two) yields

$$U = \frac{1}{2}\int_0^{2\pi}\int_0^{l}\frac{Eh}{(1-\nu^2)}\left\{\left[(\varepsilon_x + \varepsilon_\theta)^2 - 2(1-\nu)\left(\varepsilon_x\varepsilon_\theta - \frac{\varepsilon_{x\theta}^2}{4}\right)\right]\right.$$
$$+ \frac{h^2}{12}\left[(\kappa_x + \kappa_\theta)^2 - 2(1-\nu)\left(\kappa_x\kappa_\theta - \frac{\tau^2}{4}\right)\right.$$
$$\left.\left. + \frac{2}{R}(\varepsilon_x\kappa_x - \varepsilon_\theta\kappa_\theta) - \frac{(1-\nu)}{2}\frac{\varepsilon_{x\theta}}{R}\tau + \frac{\varepsilon_\theta^2}{R^2} + \frac{(1-\nu)}{2}\frac{\varepsilon_{x\theta}^2}{R^2}\right]\right\}R\,dx\,d\theta.$$

With the change of variables $s = x/R$, the total strain energy can be written as

$$U = \frac{1}{2}\int_0^{2\pi}\int_0^{l/R}\frac{Eh}{(1-\nu^2)}[I_{\mathrm{DM}} + kI_{\mathrm{BFL}}]\,ds\,d\theta\,,$$

where $k = h^2/(12R^2)$, I_{DM} is the integrand corresponding to the Donnell-Mushtari theory and I_{BFL} denotes the terms that are retained to yield the Byrne, Flügge, and Lur'ye strain energy. These two components are given by

$$I_{\mathrm{DM}} = \left(\frac{\partial u}{\partial s} + \frac{\partial v}{\partial\theta} + w\right)^2 - 2(1-\nu)\left[\frac{\partial u}{\partial s}\left(\frac{\partial v}{\partial\theta} + w\right) - \frac{1}{4}\left(\frac{\partial v}{\partial s} + \frac{\partial u}{\partial\theta}\right)^2\right]$$
$$+ k\left\{(\nabla^2 w)^2 - 2(1-\nu)\left[\frac{\partial^2 w}{\partial s^2}\frac{\partial^2 w}{\partial\theta^2} - \left(\frac{\partial^2 w}{\partial s\partial\theta}\right)^2\right]\right\}$$

and

$$I_{\mathrm{BFL}} = -2\nu\frac{\partial v}{\partial\theta}\frac{\partial^2 w}{\partial s^2} - 3(1-\nu)\frac{\partial v}{\partial s}\frac{\partial^2 w}{\partial s\partial\theta} + \frac{3}{2}(1-\nu)\left(\frac{\partial v}{\partial s}\right)^2 + (1-\nu)\frac{\partial u}{\partial\theta}\frac{\partial^2 w}{\partial s\partial\theta}$$
$$+ \frac{1}{2}(1-\nu)\left(\frac{\partial u}{\partial\theta}\right)^2 - 2\frac{\partial u}{\partial s}\frac{\partial^2 w}{\partial s^2} + 2w\frac{\partial^2 w}{\partial\theta^2} + w^2.$$

For simplicity of presentation, a weak form of the shell equations will be developed using the Donnell-Mushtari strain expression; a corresponding set of equations can be derived in a similar manner in the BFL case.

The kinetic energy of the shell is given by

$$T = \frac{1}{2}\int_0^{2\pi}\int_0^{l/R} \rho h \left[\left(\frac{\partial^2 u}{\partial t^2}\right)^2 + \left(\frac{\partial^2 v}{\partial t^2}\right)^2 + \left(\frac{\partial^2 w}{\partial t^2}\right)^2\right] R^2\, ds\, d\theta.$$

Throughout this development, it is assumed that the shell satisfies *shear diaphragm* boundary conditions at $x = 0,\ l$; that is, it is assumed that

$$v = w = N_x = M_x = 0$$

at the ends. This is done merely to demonstrate the equivalence between the weak form which follows and the strong form already discussed; other boundary conditions can be treated with similar arguments. It should be noted that the conditions $v = w = 0$ at the ends are essential boundary conditions and hence must be enforced on the chosen state space.

For an arbitrary time interval $[t_0, t_1]$, consider the action integral

$$A[\vec{u}] = \int_{t_0}^{t_1} (T - U)\, dt \tag{2.15}$$

where $\vec{u} = [u, v, w]$ is considered in the space $V = H_b^1(\Omega) \times H_b^1(\Omega) \times H_b^2(\Omega)$. Here Ω denotes the shell and the subscript b denotes the set of functions satisfying the essential boundary conditions. One then considers variations of the form

$$\hat{u} = \vec{u} + \varepsilon\vec{\Phi} = \begin{bmatrix} u(t, r, \theta, x) \\ v(t, r, \theta, x) \\ w(t, r, \theta, x) \end{bmatrix} + \varepsilon \begin{bmatrix} \eta_1(t)\phi_1(r, \theta, x) \\ \eta_2(t)\phi_2(r, \theta, x) \\ \eta_3(t)\phi_3(r, \theta, x) \end{bmatrix}.$$

Here $\vec{\eta} = [\eta_1, \eta_2, \eta_3]$ and $\vec{\phi} = [\phi_1, \phi_2, \phi_3]$ are chosen so that

(i) $\hat{u}(t, \cdot, \cdot, \cdot) \in V$, and

(ii) $\hat{u}(t_0, \cdot, \cdot, \cdot) = \hat{u}(t_1, \cdot, \cdot, \cdot)$.

Note that this enforces $\vec{\eta} \in [H^2(0, T)]^3$, $\vec{\eta}(t_0) = \vec{\eta}(t_1)$, and $\vec{\phi} \in V$.

Hamilton's principle states that the motion of the shell must give a stationary value to the action integral when compared to variations in the motion, thus leading to the requirement that, for all $\vec{\Phi}$,

$$\frac{d}{d\varepsilon} A[\vec{u} + \varepsilon\vec{\Phi}]|_{\varepsilon=0} = 0.$$

With the definition (2.15) for the action integral, Hamilton's principle leads to the

condition

$$
\begin{aligned}
0 &= \frac{\partial}{\partial \varepsilon} A[\hat{u}]|_{\varepsilon=0} \\
&= \int_{t_0}^{t_1}\int_0^{2\pi}\int_0^{l/R} \rho h\left[\frac{\partial u}{\partial t}\frac{\partial \eta_1}{\partial t}\phi_1 + \frac{\partial v}{\partial t}\frac{\partial \eta_2}{\partial t}\phi_2 + \frac{\partial w}{\partial t}\frac{\partial \eta_3}{\partial t}\phi_3\right] R^2\, ds\, d\theta\, dt \\
&\quad - \int_{t_0}^{t_1}\int_0^{2\pi}\int_0^{l/R} \frac{Eh}{(1-\nu^2)}\left\{\left(\frac{\partial u}{\partial s} + \frac{\partial v}{\partial \theta} + w\right)\left(\eta_1\frac{\partial \phi_1}{\partial s} + \eta_2\frac{\partial \phi_2}{\partial \theta} + \eta_3\phi_3\right)\right. \\
&\quad - (1-\nu)\left[\eta_1 w\frac{\partial \phi_1}{\partial s} + \eta_1\frac{\partial v}{\partial \theta}\frac{\partial \phi_1}{\partial s} + \eta_2\frac{\partial u}{\partial s}\frac{\partial \phi_2}{\partial \theta} + \eta_3\frac{\partial u}{\partial s}\phi_3\right. \\
&\qquad \left. - \frac{1}{2}\left(\frac{\partial v}{\partial s} + \frac{\partial u}{\partial \theta}\right)\left(\eta_2\frac{\partial \phi_2}{\partial s} + \eta_1\frac{\partial \phi_1}{\partial \theta}\right)\right] \\
&\quad + k\left\{\eta_3\nabla^2 w\nabla^2\phi_3 - (1-\nu)\left[\eta_3\frac{\partial^2 w}{\partial \theta^2}\frac{\partial^2 \phi_3}{\partial s^2} + \eta_3\frac{\partial^2 w}{\partial s^2}\frac{\partial^2 \phi_3}{\partial \theta^2}\right.\right. \\
&\qquad \left.\left.\left. -2\eta_3\frac{\partial^2 w}{\partial s\partial \theta}\frac{\partial^2 \phi_3}{\partial s\partial \theta}\right]\right\}\right\} ds\, d\theta\, dt.
\end{aligned}
$$

Note that this must hold for all arbitrary intervals $[t_0, t_1]$ and all admissible perturbations. Temporal integration by parts in the first integral in conjunction with the underlying condition that $\vec{\eta}(t_0) = \vec{\eta}(t_1)$ then yields the coupled system of equations

$$
\begin{aligned}
&\int_{t_0}^{t_1}\eta_1(t)\int_0^{2\pi}\int_0^{l/R}\left\{-\frac{\rho(1-\nu^2)}{E}\frac{\partial^2 u}{\partial t^2}\phi_1 R^2 - \left(\frac{\partial u}{\partial s} + \frac{\partial v}{\partial \theta} + w\right)\frac{\partial \phi_1}{\partial s}\right. \\
&\qquad \left. +(1-\nu)\left[w\frac{\partial \phi_1}{\partial s} + \frac{\partial v}{\partial \theta}\frac{\partial \phi_1}{\partial s} - \frac{1}{2}\left(\frac{\partial v}{\partial s} + \frac{\partial u}{\partial \theta}\right)\frac{\partial \phi_1}{\partial \theta}\right]\right\} ds\, d\theta\, dt = 0,
\end{aligned}
$$

$$
\begin{aligned}
&\int_{t_0}^{t_1}\eta_2(t)\int_0^{2\pi}\int_0^{l/R}\left\{-\frac{\rho(1-\nu^2)}{E}\frac{\partial^2 v}{\partial t^2}\phi_2 R^2 - \left(\frac{\partial u}{\partial s} + \frac{\partial v}{\partial \theta} + w\right)\frac{\partial \phi_2}{\partial \theta}\right. \\
&\qquad \left. +(1-\nu)\left[\frac{\partial u}{\partial s}\frac{\partial \phi_2}{\partial \theta} - \frac{1}{2}\left(\frac{\partial v}{\partial s} + \frac{\partial u}{\partial \theta}\right)\frac{\partial \phi_2}{\partial s}\right]\right\} ds\, d\theta\, dt = 0,
\end{aligned}
$$

$$
\begin{aligned}
&\int_{t_0}^{t_1}\eta_3(t)\int_0^{2\pi}\int_0^{l/R}\left\{-\frac{\rho(1-\nu^2)}{E}\frac{\partial^2 w}{\partial t^2}\phi_3 R^2 - \left(\frac{\partial u}{\partial s} + \frac{\partial v}{\partial \theta} + w\right)\phi_3 + (1-\nu)\frac{\partial u}{\partial s}\phi_3\right. \\
&\left. -k\left\{\nabla^2 w\nabla^2\phi_3 - (1-\nu)\left[\frac{\partial^2 w}{\partial \theta^2}\frac{\partial^2 \phi_3}{\partial s^2} + \frac{\partial^2 w}{\partial s^2}\frac{\partial^2 \phi_3}{\partial \theta^2} - 2\frac{\partial^2 w}{\partial s\partial \theta}\frac{\partial^2 \phi_3}{\partial s\partial \theta}\right]\right\}\right\} ds\, d\theta\, dt = 0.
\end{aligned}
$$

The weak form of the equations of motion for the unforced shell is thus

$$\int_0^{2\pi}\int_0^{l/R}\left\{\frac{R^2}{C_L^2}\frac{\partial^2 u}{\partial t^2}\phi_1+\left(\frac{\partial u}{\partial s}+\nu\frac{\partial v}{\partial\theta}+\nu w\right)\frac{\partial\phi_1}{\partial s}\right.$$
$$\left.+\frac{1}{2}(1-\nu)\left(\frac{\partial v}{\partial s}+\frac{\partial u}{\partial\theta}\right)\frac{\partial\phi_1}{\partial\theta}\right\}ds\,d\theta=0,$$

$$\int_0^{2\pi}\int_0^{l/R}\left\{\frac{R^2}{C_L^2}\frac{\partial^2 v}{\partial t^2}\phi_2+\left(\nu\frac{\partial u}{\partial s}+\frac{\partial v}{\partial\theta}+w\right)\frac{\partial\phi_2}{\partial\theta}\right.$$
$$\left.+\frac{1}{2}(1-\nu)\left(\frac{\partial v}{\partial s}+\frac{\partial u}{\partial\theta}\right)\frac{\partial\phi_2}{\partial s}\right\}ds\,d\theta=0,$$

$$\int_0^{2\pi}\int_0^{l/R}\left\{\frac{R^2}{C_L^2}\frac{\partial^2 w}{\partial t^2}\phi_3+\left(\nu\frac{\partial u}{\partial s}+\frac{\partial v}{\partial\theta}+w\right)\phi_3\right.$$
$$\left.+k\left\{\nabla^2 w\nabla^2\phi_3-(1-\nu)\left[\frac{\partial^2 w}{\partial\theta^2}\frac{\partial^2\phi_3}{\partial s^2}+\frac{\partial^2 w}{\partial s^2}\frac{\partial^2\phi_3}{\partial\theta^2}-2\frac{\partial^2 w}{\partial s\partial\theta}\frac{\partial^2\phi_3}{\partial s\partial\theta}\right]\right\}\right\}ds\,d\theta=0$$

for all $\vec{\phi}\in V$. Again, the constant $C_L=[E/(\rho(1-\nu^2))]^{1/2}$ is the phase speed of axial waves in the cylinder wall.

In terms of the moment and force resultants (see (2.9)) and the original axial variable x, the weak form is

$$\int_0^{2\pi}\int_0^{l}\left\{Rph\frac{\partial^2 u}{\partial t^2}\phi_1+RN_x\frac{\partial\phi_1}{\partial x}+N_{\theta x}\frac{\partial\phi_1}{\partial\theta}\right\}dx\,d\theta=0,$$

$$\int_0^{2\pi}\int_0^{l}\left\{Rph\frac{\partial^2 v}{\partial t^2}\phi_2+N_\theta\frac{\partial\phi_2}{\partial\theta}+RN_{x\theta}\frac{\partial\phi_2}{\partial x}\right\}dx\,d\theta=0,\tag{2.16}$$

$$\int_0^{2\pi}\int_0^{l}\left\{Rph\frac{\partial^2 w}{\partial t^2}\phi_3+N_\theta\phi_3-RM_x\frac{\partial^2\phi_3}{\partial x^2}-\frac{1}{R}M_\theta\frac{\partial^2\phi_3}{\partial\theta^2}-2M_{x\theta}\frac{\partial^2\phi_3}{\partial x\partial\theta}\right\}dx\,d\theta=0.$$

The derivation thus far has been for the unforced shell. To include the contributions of applied external forces and moments that do nonconservative work on the shell, one can appeal to an extended form of Hamilton's principle or more formally include these contributions directly in the system (2.16). Both techniques yield identical final equations, and for ease of presentation we will take the latter approach.

The inclusion of the applied line forces and moments $\hat{N}_x$, $\hat{N}_\theta$ and $\hat{M}_x$, $\hat{M}_\theta$ and the surface load $\hat{q}_n$ in the system then yields

$$\begin{aligned}
&\int_0^{2\pi}\int_0^l \left\{ R\rho h\frac{\partial^2 u}{\partial t^2}\phi_1 + RN_x\frac{\partial \phi_1}{\partial x} + N_{\theta x}\frac{\partial \phi_1}{\partial \theta} - R\hat{N}_x\frac{\partial \phi_1}{\partial x}\right\} dx\, d\theta = 0,\\
&\int_0^{2\pi}\int_0^l \left\{ R\rho h\frac{\partial^2 v}{\partial t^2}\phi_2 + N_\theta\frac{\partial \phi_2}{\partial \theta} + RN_{x\theta}\frac{\partial \phi_2}{\partial x} - \hat{N}_x\frac{\partial \phi_2}{\partial \theta}\right\} dx\, d\theta = 0,\\
&\int_0^{2\pi}\int_0^l \left\{ R\rho h\frac{\partial^2 w}{\partial t^2}\phi_3 + N_\theta\phi_3 - RM_x\frac{\partial^2 \phi_3}{\partial x^2} - \frac{1}{R}M_\theta\frac{\partial^2 \phi_3}{\partial \theta^2} - 2M_{x\theta}\frac{\partial^2 \phi_3}{\partial x\partial \theta}\right.\\
&\qquad\left. - R\hat{q}_n\phi_3 + R\hat{M}_x\frac{\partial^2 \phi_3}{\partial x^2} + \frac{1}{R}\hat{M}_\theta\frac{\partial^2 \phi_3}{\partial \theta^2}\right\} dx\, d\theta = 0
\end{aligned} \tag{2.17}$$

for all $\vec{\phi} \in V$ as the weak form of the Donnell-Mushtari equations of motion for the forced shell.

With the assumption of sufficient smoothness, the weak solution in this form is consistent with the strong solution in (2.12). The vanishing of several of the boundary terms that arise during integration by parts is a result of the choice $V = H_b^1(\Omega) \times H_b^1(\Omega) \times H_b^2(\Omega)$ for the function space since the state variables and test functions are required to satisfy the essential boundary conditions

$$v = w = 0$$

at $x = 0, l$.

We point out that in the weak form (2.17), one is not required to differentiate the applied force and moment resultants $\hat{N}_x$, $\hat{N}_\theta$, $\hat{M}_x$, and $\hat{M}_\theta$ as is required in the strong form (2.14). This proves to be very beneficial when these terms are generated by finite piezoceramic patches, as discussed in the next section.

Plate equations. Consider a thin rectangular plate whose edges lie along the coordinate lines $x = 0, l$ and $y = 0, a$. We assume that the plate is subjected to both longitudinal and transverse loading via the surface forces and moments $\hat{q}_x$, $\hat{q}_\theta$, $\hat{q}_n$ and $\hat{m}_x$, $\hat{m}_\theta$. With u, v, and w denoting the displacements in the x, y, and normal directions, respectively, the strong form of the Kirchhoff plate equations is given by

$$\begin{aligned}
&\rho h\frac{\partial^2 u}{\partial t^2} - \frac{\partial N_x}{\partial x} - \frac{\partial N_{yx}}{\partial y} = \hat{q}_x,\\
&\rho h\frac{\partial^2 v}{\partial t^2} - \frac{\partial N_y}{\partial y} - \frac{\partial N_{xy}}{\partial x} = \hat{q}_y,\\
&\rho h\frac{\partial^2 w}{\partial t^2} - \frac{\partial^2 M_x}{\partial x^2} - \frac{\partial^2 M_y}{\partial y^2} - \frac{\partial^2 M_{xy}}{\partial x\partial y} - \frac{\partial^2 M_{yx}}{\partial y\partial x} = \hat{q}_n + \frac{\partial \hat{m}_x}{\partial y} + \frac{\partial \hat{m}_y}{\partial x},
\end{aligned} \tag{2.18}$$

where the moment and force resultants are

$$N_x = \frac{Eh}{1-\nu^2}\left(\frac{\partial u}{\partial x} + \nu\frac{\partial v}{\partial y}\right), \qquad M_x = -\frac{Eh^3}{12(1-\nu^2)}\left(\frac{\partial^2 w}{\partial x^2} + \nu\frac{\partial^2 w}{\partial y^2}\right),$$

$$N_y = \frac{Eh}{1-\nu^2}\left(\frac{\partial v}{\partial y} + \nu\frac{\partial u}{\partial x}\right), \qquad M_y = -\frac{Eh^3}{12(1-\nu^2)}\left(\frac{\partial^2 w}{\partial y^2} + \nu\frac{\partial^2 w}{\partial x^2}\right),$$

$$N_{xy} = N_{yx} = \frac{Eh}{2(1+\nu)}\left(\frac{\partial v}{\partial x} + \frac{\partial u}{\partial y}\right), \quad M_{xy} = M_{yx} = -\frac{Eh^3}{12(1+\nu)}\frac{\partial^2 w}{\partial x \partial y}.$$

The first two equations in (2.18) describe the longitudinal movement of the plate while the third equation describes the transverse motion of the plate.

To find the weak form of the equations, the vector $\vec{u} = [u, v, w]$ containing the displacements in the x, y, and normal directions is considered in the space $V = H_b^1(\Omega) \times H_b^1(\Omega) \times H_b^2(\Omega)$, where Ω denotes the plate and the subscript b denotes the set of functions satisfying essential boundary conditions for a specific problem. By using analysis similar to that just described for cylindrical shells, the weak form of the equations of motion for the plate can be found to be

$$\begin{aligned}
&\int_0^a \int_0^l \left\{ \rho h \frac{\partial^2 u}{\partial t^2}\phi_1 + N_x \frac{\partial \phi_1}{\partial x} + N_{yx}\frac{\partial \phi_1}{\partial y} - \hat{N}_x \frac{\partial \phi_1}{\partial x} \right\} dx\, dy = 0, \\
&\int_0^a \int_0^l \left\{ \rho h \frac{\partial^2 v}{\partial t^2}\phi_2 + N_y \frac{\partial \phi_2}{\partial y} + N_{xy}\frac{\partial \phi_2}{\partial x} - \hat{N}_y \frac{\partial \phi_2}{\partial y} \right\} dx\, dy = 0, \\
&\int_0^a \int_0^l \left\{ \rho h \frac{\partial^2 w}{\partial t^2}\phi_3 - M_x \frac{\partial^2 \phi_3}{\partial x^2} - M_y \frac{\partial^2 \phi_3}{\partial y^2} - M_{xy}\frac{\partial^2 \phi_3}{\partial x \partial y} \right. \\
&\qquad \left. - M_{yx}\frac{\partial^2 \phi_3}{\partial x \partial y} - \hat{q}_n \phi_3 + \widehat{M}_x \frac{\partial^2 \phi_3}{\partial x^2} + \widehat{M}_y \frac{\partial^2 \phi_3}{\partial y^2} \right\} dx\, dy = 0
\end{aligned} \tag{2.19}$$

for all $\vec{\phi} = [\phi_1, \phi_2, \phi_3] \in V$. As in the case of the thin shell, the external line forces and moments $\hat{N}_x$, $\hat{N}_y$, $\widehat{M}_x$, and $\widehat{M}_y$ are related in an infinitesimal sense to the corresponding area forces and moments $\hat{q}_x$, $\hat{q}_y$, $\hat{m}_y$, and $\hat{m}_x$ appearing in the strong form of the equations by the relations

$$\hat{q}_x = -\frac{\partial \hat{N}_x}{\partial x}, \quad \hat{q}_y = -\frac{\partial \hat{N}_y}{\partial y}, \quad \hat{m}_x = -\frac{\partial \widehat{M}_y}{\partial y}, \quad \hat{m}_y = -\frac{\partial \widehat{M}_x}{\partial x}. \tag{2.20}$$

If the solution has sufficient smoothness, integration by parts can be used to show that the weak solution is consistent with the strong solution in (2.18).

Beam equations. The motion of an undamped thin beam of length l and width b can be determined from the dynamics of thin plate theory by considering only the vibrations in the x direction along with the usual transverse vibrations (in the z direction). From (2.18) this yields the strong form of the Euler-Bernoulli beam equations

$$\rho h b \frac{\partial^2 u}{\partial t^2} - \frac{\partial N_x}{\partial x} = \hat{q}_x, \qquad \rho h b \frac{\partial^2 w}{\partial t^2} - \frac{\partial^2 M_x}{\partial x^2} = \hat{q}_n + \frac{\partial \hat{m}_y}{\partial x}, \tag{2.21}$$

where

$$N_x = Ehb\frac{\partial u}{\partial x},$$

$$M_x = -\frac{Eh^3b}{12}\frac{\partial^2 w}{\partial x^2} = -EI\frac{\partial^2 w}{\partial x^2}.$$

Note that $I = h^3b/12$ is the moment of inertia for a beam of width b and thickness h.

A corresponding weak or variational form of the equations can be determined by choosing $V = H_b^1(\Omega) \times H_b^2(\Omega)$ for the space of trial functions, where Ω denotes the beam and the subscript b again denotes the set of functions that must satisfy the essential boundary conditions. Through either an energy derivation such as that given for the thin shell, or simply integration by parts, one arrives at the variational form

$$\int_0^l \left\{ \rho hb\frac{\partial^2 u}{\partial t^2}\phi_1 + N_x\frac{\partial \phi_1}{\partial x} - \hat{N}_x\frac{\partial \phi_1}{\partial x} \right\} dx = 0 \quad \text{for all } \phi_1 \in H_b^1(\Omega),$$

$$\int_0^l \left\{ \rho hb\frac{\partial^2 w}{\partial t^2}\phi_3 - M_x\frac{\partial^2 \phi_3}{\partial x^2} - \hat{q}_n\phi_3 + \hat{M}_x\frac{\partial^2 \phi_3}{\partial x^2} \right\} dx = 0 \quad \text{for all } \phi_3 \in H_b^2(\Omega) \tag{2.22}$$

of the beam equations. We point out that in this form one is not required to differentiate the external force or moment resultants, $\hat{N}_x$ and $\hat{M}_x$, which proves to be very useful when these terms are generated by the activation of finite piezoceramic patches.

3. Patch contributions to the shell equations. In the last section, the strong and weak forms of the equations of motion for a homogeneous, thin cylindrical shell having uniform thickness were presented (see (2.12) and (2.17)). When piezoceramic patches are bonded to the shell, these basic equations are affected in two ways. First, the presence of the patches on the shell significantly alters the material properties and thickness of the structure in regions covered by the patches; this must be taken into account when determining the internal (material) moment and force resultants to be used in (2.12) and (2.17). Moreover, when a voltage is applied, mechanical strains are induced in the patches, which leads to external moments and forces as loads in the shell model. Both contributions are discussed here, and a general model describing the structural dynamics when patches are bonded to the shell is presented.

We assume for now that a pair of piezoceramic patches having thickness T are perfectly bonded to a cylindrical shell of thickness h with midsurface radius R (see Fig. 3). As shown in Fig. 4, the patches are assumed to be situated so that their edges are parallel to lines of constant x and θ.

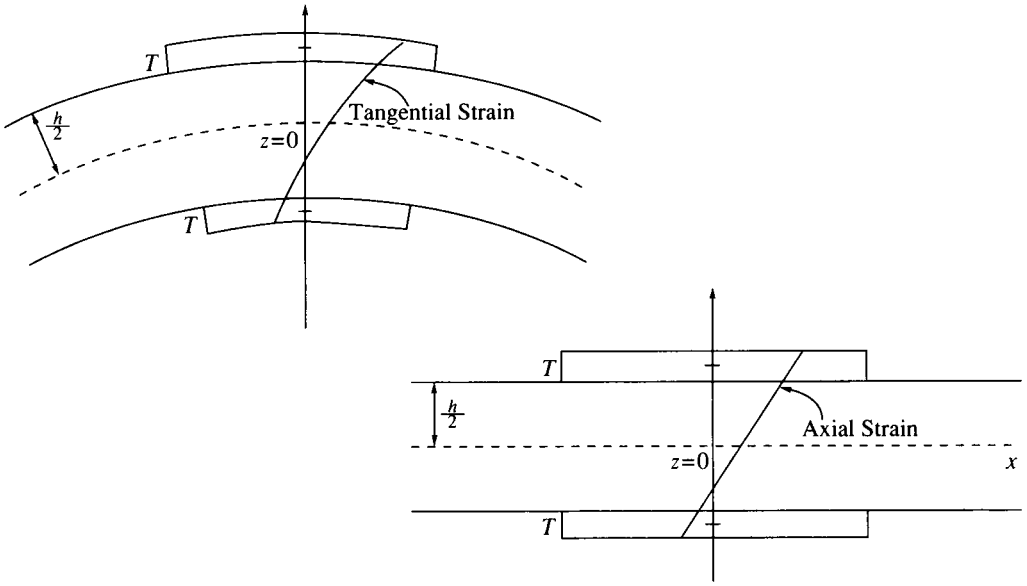

FIG. 3. Strain distribution for the composite structure

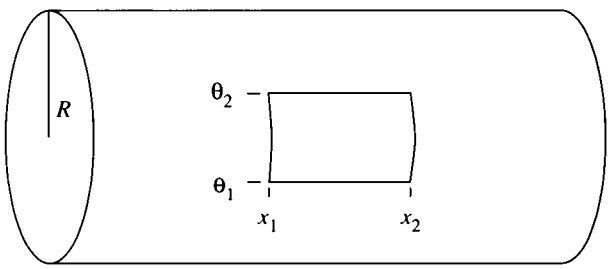

FIG. 4. Piezoceramic patch placement

Internal forces and moments. As noted in (2.1), the infinitesimally exact strain relationships for a cylindrical shell having midsurface radius R are given by

$$e_x = (\varepsilon_x + z\kappa_x),$$
$$e_\theta = \frac{1}{(1 + z/R)}(\varepsilon_\theta + z\kappa_\theta),$$
$$\gamma_{x\theta} = \frac{1}{(1 + z/R)}\left[\varepsilon_{x\theta} + z\left(1 + \frac{z}{2R}\right)\tau\right]$$

with ε_x, ε_θ, κ_x, κ_θ, $\varepsilon_{x\theta}$, and τ described in (2.3). To simplify the discussion that follows, we will neglect the term z/R with respect to unity as is done in the Donnell-Mushtari theory; we emphasize, however, that this is done merely for brevity of presentation and the infinitesimally exact terms can be used in a manner corresponding to that of the Byrne-Flügge-Lur'ye theory. Moreover, it is reasonable to assume that this relationship is maintained throughout the combined thickness $h + 2T$ as shown in Fig. 3 (see [13]). Hence we will take $e_x = \varepsilon_x + z\kappa_x$, $e_\theta = \varepsilon_\theta + z\kappa_\theta$, and $\gamma_{x\theta} = \varepsilon_{x\theta} + z\tau$ throughout the combined thickness of the structure. Note that this assumption implies that the strains at the interface are continuous and that the centers for the radii of curvature for the shell and patch are concurrent.

Although the same strain distribution is assumed throughout the patch and shell, the stress changes since the Young's modulus and Poisson ratio for the patch will, in general, differ from those of the shell. For an undamped shell with E_1, ν_1 and E_2, ν_2 denoting the Young's modulus and Poisson ratio for the outer and inner patches, respectively, the stress component σ_x is given by

$$\sigma_x = \begin{cases} \dfrac{E}{1-\nu^2}(e_x + \nu e_\theta) & \text{(shell)}, \\ \dfrac{E_1}{1-\nu_1^2}(e_x + \nu_1 e_\theta) & \text{(outer patch)}, \\ \dfrac{E_2}{1-\nu_2^2}(e_x + \nu_2 e_\theta) & \text{(inner patch)}, \end{cases} \tag{3.1}$$

with similar expressions for σ_θ and $\sigma_{x\theta} = \sigma_{\theta x}$ (see (2.4)). The subscripts 1 and 2 will be used throughout this discussion to denote outer and inner patch properties, respectively.

The moment and force resultants are obtained by integrating the stresses across the thickness of the structure. This yields the expressions

$$\begin{bmatrix} N_x \\ N_{x\theta} \end{bmatrix} = \int_{-h/2-T}^{h/2+T} \begin{bmatrix} \sigma_x \\ \sigma_{x\theta} \end{bmatrix} \left(1 + \frac{z}{R}\right) dz, \qquad \begin{bmatrix} N_\theta \\ N_{\theta x} \end{bmatrix} = \int_{-h/2-T}^{h/2+T} \begin{bmatrix} \sigma_\theta \\ \sigma_{\theta x} \end{bmatrix} dz$$

$$\begin{bmatrix} M_x \\ M_{x\theta} \end{bmatrix} = \int_{-h/2-T}^{h/2+T} \begin{bmatrix} \sigma_x \\ \sigma_{x\theta} \end{bmatrix} \left(1 + \frac{z}{R}\right) z\, dz, \qquad \begin{bmatrix} M_\theta \\ M_{\theta x} \end{bmatrix} = \int_{-h/2-T}^{h/2+T} \begin{bmatrix} \sigma_\theta \\ \sigma_{\theta x} \end{bmatrix} z\, dz \tag{3.2}$$

in regions of the structure covered by the patches and the previously discussed expressions (2.5)–(2.8) in those regions of the structure consisting solely of shell material. In accordance with the Donnell-Mushtari assumptions, the curvature terms z/R appearing in the integrals are neglected with respect to unity, but again, this is done for ease of presentation and higher-order results can be obtained by retaining these terms. For the *undamped combined* structure when *both patches* in a pair are present and have *potentially differing material properties*, this yields the force and moment

resultants

$$
\begin{aligned}
N_x &= \frac{Eh}{1-\nu^2}(\varepsilon_x + \nu\varepsilon_\theta) + \frac{E_1}{1-\nu_1^2}\left[(\varepsilon_x + \nu_1\varepsilon_\theta)T + \frac{a_2}{2}(\kappa_x + \nu_1\kappa_\theta)\right]\chi_{pe}(x,\theta) \\
&\quad + \frac{E_2}{1-\nu_2^2}\left[(\varepsilon_x + \nu_2\varepsilon_\theta)T - \frac{a_2}{2}(\kappa_x + \nu_2\kappa_\theta)\right]\chi_{pe}(x,\theta), \\
N_\theta &= \frac{Eh}{1-\nu^2}(\varepsilon_\theta + \nu\varepsilon_x) + \frac{E_1}{1-\nu_1^2}\left[(\varepsilon_\theta + \nu_1\varepsilon_x)T + \frac{a_2}{2}(\kappa_\theta + \nu_1\kappa_x)\right]\chi_{pe}(x,\theta) \\
&\quad + \frac{E_2}{1-\nu_2^2}\left[(\varepsilon_\theta + \nu_2\varepsilon_x)T - \frac{a_2}{2}(\kappa_\theta + \nu_2\kappa_x)\right]\chi_{pe}(x,\theta), \\
N_{x\theta} &= N_{\theta x} = \frac{Eh}{2(1+\nu)}\varepsilon_{x\theta} + E_1\left[\frac{T}{2(1+\nu_1)}\varepsilon_{x\theta} + \frac{a_2}{4(1+\nu_1)}\tau\right]\chi_{pe}(x,\theta) \\
&\quad + E_2\left[\frac{T}{2(1+\nu_2)}\varepsilon_{x\theta} - \frac{a_2}{4(1+\nu_2)}\tau\right]\chi_{pe}(x,\theta), \\
M_x &= \frac{Eh^3}{12(1-\nu^2)}(\kappa_x + \nu\kappa_\theta) + \frac{E_1}{1-\nu_1^2}\left[(\varepsilon_x + \nu_1\varepsilon_\theta)\frac{a_2}{2} + (\kappa_x + \nu_1\kappa_\theta)\frac{a_3}{3}\right]\chi_{pe}(x,\theta) \\
&\quad + \frac{E_2}{1-\nu_2^2}\left[-(\varepsilon_x + \nu_2\varepsilon_\theta)\frac{a_2}{2} + (\kappa_x + \nu_2\kappa_\theta)\frac{a_3}{3}\right]\chi_{pe}(x,\theta), \\
M_\theta &= \frac{Eh^3}{12(1-\nu^2)}(\kappa_\theta + \nu\kappa_x) + \frac{E_1}{1-\nu_1^2}\left[(\varepsilon_\theta + \nu_1\varepsilon_x)\frac{a_2}{2} + (\kappa_\theta + \nu_1\kappa_x)\frac{a_3}{3}\right]\chi_{pe}(x,\theta) \\
&\quad + \frac{E_2}{1-\nu_2^2}\left[-(\varepsilon_\theta + \nu_2\varepsilon_x)\frac{a_2}{2} + (\kappa_\theta + \nu_2\kappa_x)\frac{a_3}{3}\right]\chi_{pe}(x,\theta), \\
M_{x\theta} &= M_{\theta x} = \frac{Eh^3}{24(1+\nu)}\tau + E_1\left[\frac{a_2}{4(1+\nu_1)}\varepsilon_{x\theta} + \frac{a_3}{6(1+\nu_1)}\tau\right]\chi_{pe}(x,\theta) \\
&\quad + E_2\left[-\frac{a_2}{4(1+\nu_2)}\varepsilon_{x\theta} + \frac{a_3}{6(1+\nu_2)}\tau\right]\chi_{pe}(x,\theta).
\end{aligned}
\tag{3.3}
$$

The constants a_2 and a_3 are given by

$$
a_2 = \left(\frac{h}{2} + T\right)^2 - \frac{h^2}{4}, \qquad a_3 = \left(\frac{h}{2} + T\right)^3 - \frac{h^3}{8},
$$

while the characteristic function $\chi_{pe}(x,\theta)$ has the definition

$$
\chi_{pe}(x,\theta) = \begin{cases} 1, & x_1 \le x \le x_2,\ \theta_1 \le \theta \le \theta_2, \\ 0, & \text{otherwise.} \end{cases}
$$

The midsurface characteristics ε_x, ε_θ, κ_x, κ_θ, $\varepsilon_{x\theta}$, and τ are described in (2.3).

In the case where *both patches* have *identical material properties* ($E_2 = E_1$ and $\nu_2 = \nu_1$), these expressions simplify to yield

$$
\begin{aligned}
N_x &= \frac{Eh}{1-\nu^2}(\varepsilon_x + \nu\varepsilon_\theta) + \frac{2E_1T}{1-\nu_1^2}(\varepsilon_x + \nu_1\varepsilon_\theta)\chi_{pe}(x,\theta),\\
N_\theta &= \frac{Eh}{1-\nu^2}(\varepsilon_\theta + \nu\varepsilon_x) + \frac{2E_1T}{1-\nu_1^2}(\varepsilon_\theta + \nu_1\varepsilon_x)\chi_{pe}(x,\theta),\\
N_{x\theta} &= N_{\theta x} = \frac{Eh}{2(1+\nu)}\varepsilon_{x\theta} + \frac{E_1T}{(1+\nu_1)}\varepsilon_{x\theta}\chi_{pe}(x,\theta),\\
M_x &= \frac{Eh^3}{12(1-\nu^2)}(\kappa_x + \nu\kappa_\theta) + \frac{2E_1a_3}{3(1-\nu_1^2)}(\kappa_x + \nu_1\kappa_\theta)\chi_{pe}(x,\theta),\\
M_\theta &= \frac{Eh^3}{12(1-\nu^2)}(\kappa_\theta + \nu\kappa_x) + \frac{2E_1a_3}{3(1-\nu_1^2)}(\kappa_\theta + \nu_1\kappa_x)\chi_{pe}(x,\theta),\\
M_{x\theta} &= M_{\theta x} = \frac{Eh^3}{24(1+\nu)}\tau + \frac{E_1a_3}{3(1+\nu_1)}\tau\chi_{pe}(x,\theta).
\end{aligned}
\tag{3.4}
$$

If only *one* patch is present, the internal force and moment resultants for the structure can be determined from (3.3) by omitting the contributions from the missing patch. For example, if only an outer patch is bonded to the shell, one can obtain the internal resultants for the structure by deleting those terms in (3.3) that are multiplied by E_2.

Finally, internal Kelvin-Voigt damping can be incorporated in the model by assuming a more general constitutive relation in which stress is taken to be proportional to a linear combination of strain and strain rate. Letting c_D, c_{D_1}, and c_{D_2} denote the damping coefficients in the shell, outer patch, and inner patch, respectively, we can replace the stress component σ_x in (3.1) by the more general expression

$$
\sigma_x = \begin{cases}
\dfrac{E}{1-\nu^2}(e_x + \nu e_\theta) + \dfrac{c_D}{1-\nu^2}(\dot{e}_x + \nu\dot{e}_\theta) & \text{(shell)},\\
\dfrac{E_1}{1-\nu_1^2}(e_x + \nu_1 e_\theta) + \dfrac{c_{D_1}}{1-\nu_1^2}(\dot{e}_x + \nu_1\dot{e}_\theta) & \text{(outer patch)},\\
\dfrac{E_2}{1-\nu_2^2}(e_x + \nu_2 e_\theta) + \dfrac{c_{D_2}}{1-\nu_2^2}(\dot{e}_x + \nu_2\dot{e}_\theta) & \text{(inner patch)},
\end{cases}
$$

with analogous expressions for σ_θ and $\sigma_{x\theta}$. The substitution of these stress terms into (3.2) then yields moment and force expressions analogous to those in (3.3) and (3.4) but, which now include damping contributions containing the temporal derivatives of the terms ε_x, ε_θ, κ_x, κ_θ, $\varepsilon_{x\theta}$, and τ given in (2.3).

The internal moments and forces determined by (3.3) and (3.4) are then substituted into (2.12) if one is using the strong form of the shell equations, or (2.17) if one is employing the weak form of the equations. In this manner, the material contributions due to the presence of the piezoceramic patches are incorporated in the dynamic equations of motion.

External moments and forces. The second contribution from the piezoceramic patches is the generation of external moments and forces which results from the

property that when a voltage is applied, mechanical strains are induced in the x and θ directions. Here we assume that when the patch is activated, in accordance with basic shell theory, equal strains are induced in the x and θ directions and the radius of curvature is not changed in either direction. Patches satisfying this assumption could be made, for example, by taking a portion of a thin-walled tubular piezoceramic element.

The magnitude of the induced free strains is taken to be

$$e_{pe_1} = (e_x)_{pe_1} = (e_\theta)_{pe_1} = \frac{d_{31}}{T} V_1,$$
$$e_{pe_2} = (e_x)_{pe_2} = (e_\theta)_{pe_2} = \frac{d_{31}}{T} V_2,$$

where d_{31} is a piezoceramic strain constant, and V_1 and V_2 are the applied voltages into the outer and inner patches, respectively. We point out that when a voltage is applied to a patch with edge coordinates x_1, x_2, θ_1, and θ_2, the point $(\bar{x}, \bar{\theta}) = ((x_1 + x_2)/2,\ R(\theta_1 + \theta_2)/2)$ will not move whereas the axially symmetric points on either side will move an equal amount in opposite directions. This observation is important when determining the sense of the force resultants, and it motivates the use of indicator functions in several of the following expressions.

With E_1, ν_1 and E_2, ν_2 again denoting the Young's modulus and Poisson ratio for the outer and inner patch, respectively, the induced external stress distribution in the individual patches is taken to be

$$\begin{aligned}(\sigma_x)_{pe_1} &= (\sigma_\theta)_{pe_1} = -\frac{E_1}{1-\nu_1} e_{pe_1},\\ (\sigma_x)_{pe_2} &= (\sigma_\theta)_{pe_2} = -\frac{E_2}{1-\nu_2} e_{pe_2}.\end{aligned} \tag{3.5}$$

The negative signs result from the conservation of forces when balancing the material and induced stresses in the patch.

By integrating the stresses over the face of a fundamental element, it follows that the external moment and force resultants due to the activation of the individual patches can be expressed as

$$(M_x)_{pe_1} = \int_{h/2}^{h/2+T} (\sigma_x)_{pe_1} \left(1 + \frac{z}{R}\right) z\, dz, \quad (M_x)_{pe_2} = \int_{-h/2-T}^{-h/2} (\sigma_x)_{pe_2} \left(1 + \frac{z}{R}\right) z\, dz,$$
$$(M_\theta)_{pe_1} = \int_{h/2}^{h/2+T} (\sigma_\theta)_{pe_1} z\, dz, \qquad (M_\theta)_{pe_2} = \int_{-h/2-T}^{-h/2} (\sigma_\theta)_{pe_2} z\, dz,$$
$$(N_x)_{pe_1} = \int_{h/2}^{h/2+T} (\sigma_x)_{pe_1} \left(1 + \frac{z}{R}\right) dz, \quad (N_x)_{pe_2} = \int_{-h/2-T}^{-h/2} (\sigma_x)_{pe_2} \left(1 + \frac{z}{R}\right) dz,$$
$$(N_\theta)_{pe_1} = \int_{h/2}^{h/2+T} (\sigma_\theta)_{pe_1} dz, \qquad (N_\theta)_{pe_2} = \int_{-h/2-T}^{-h/2} (\sigma_\theta)_{pe_2} dz$$

with units of moment per unit length and force per unit length, respectively. Inte-

gration then yields the external forces and moments

$$
\begin{aligned}
(M_x)_{pe_1} &= -\frac{E_1}{1-\nu_1}\left[\frac{1}{8}\left(4\left(\frac{h}{2}+T\right)^2-h^2\right)+\frac{1}{R}\frac{1}{24}\left(8\left(\frac{h}{2}+T\right)^3-h^3\right)\right]e_{pe_1},\\
(M_x)_{pe_2} &= \frac{E_2}{1-\nu_2}\left[\frac{1}{8}\left(4\left(\frac{h}{2}+T\right)^2-h^2\right)-\frac{1}{R}\frac{1}{24}\left(8\left(\frac{h}{2}+T\right)^3-h^3\right)\right]e_{pe_2},\\
(M_\theta)_{pe_1} &= -\frac{E_1}{1-\nu_1}\left[\frac{1}{8}\left(4\left(\frac{h}{2}+T\right)^2-h^2\right)\right]e_{pe_1},\\
(M_\theta)_{pe_2} &= \frac{E_2}{1-\nu_2}\left[\frac{1}{8}\left(4\left(\frac{h}{2}+T\right)^2-h^2\right)\right]e_{pe_2},\\
(N_x)_{pe_1} &= -\frac{E_1}{1-\nu_1}\left[T+\frac{1}{R}\frac{1}{8}\left(4\left(\frac{h}{2}+T\right)^2-h^2\right)\right]e_{pe_1},\\
(N_x)_{pe_2} &= -\frac{E_2}{1-\nu_2}\left[T-\frac{1}{R}\frac{1}{8}\left(4\left(\frac{h}{2}+T\right)^2-h^2\right)\right]e_{pe_2},\\
(N_\theta)_{pe_1} &= -\frac{E_1}{1-\nu_1}Te_{pe_1},\\
(N_\theta)_{pe_2} &= -\frac{E_2}{1-\nu_2}Te_{pe_1}.
\end{aligned}
\tag{3.6}
$$

We note that in evaluating these integrals, we have retained the terms z/R that result from the curvature of the shell. Although this yields external terms having slightly more accuracy than the internal resultants obtained via the Donnell-Mushtari assumptions, it provides expressions for the loads due to the excitation of the individual patches that can be directly used in higher-order theories (e.g., the Byrne-Flügge-Lur'ye theory) without alteration.

We also emphasize that the expressions in (3.6) admit differing voltages into the patches, including the possibility of letting one patch remain passive with no voltage being applied. This provides a great deal of flexibility in applying various types of loads through the activation of the patches.

Thus far in the development of the external forces and moments due to the activation of the patches, edge effects have been ignored, and hence the expressions in (3.6) apply to patches covering the full circumference of the shell and having infinite axial length. The equations can be modified for finite patches in the following manner. For a patch with bounding values x_1, x_2, θ_1, and θ_2 as shown in Fig. 4, the total line moments and forces are

$$
\begin{aligned}
(M_x)_{pe} &= [(M_x)_{pe_1}+(M_x)_{pe_2}][H_1(x)-H_2(x)][H_1(\theta)-H_2(\theta)],\\
(M_\theta)_{pe} &= [(M_\theta)_{pe_1}+(M_\theta)_{pe_2}][H_1(x)-H_2(x)][H_1(\theta)-H_2(\theta)],\\
(N_x)_{pe} &= [(N_x)_{pe_1}+(N_x)_{pe_2}][H_1(x)-H_2(x)][H_1(\theta)-H_2(\theta)]S_{1,2}(x)\widehat{S}_{1,2}(\theta),\\
(N_\theta)_{pe} &= [(N_\theta)_{pe_1}+(N_\theta)_{pe_2}][H_1(x)-H_2(x)][H_1(\theta)-H_2(\theta)]S_{1,2}(x)\widehat{S}_{1,2}(\theta),
\end{aligned}
\tag{3.7}
$$

where H is the Heaviside function and $H_i(x) \equiv H(x-x_i)$, $i=1,2$, with a similar

definition in θ. The presence of the indicator function

$$S_{1,2}(x) = \begin{cases} 1, & x < (x_1 + x_2)/2, \\ 0, & x = (x_1 + x_2)/2, \\ -1, & x > (x_1 + x_2)/2 \end{cases} \tag{3.8}$$

(with an analogous definition for $\hat{S}_{1,2}(\theta)$), derives from the property that for homogeneous patches having uniform thickness, opposite but equal strains are generated about the point $(\bar{x}, \bar{\theta}) = ((x_1+x_2)/2, R(\theta_1+\theta_2)/2)$ in the two coordinate directions.

If the weak form (2.17) is used, the external line moments and forces are simply

$$\hat{M}_x = (M_x)_{pe}, \quad \hat{M}_\theta = (M_\theta)_{pe}, \quad \hat{N}_x = (N_x)_{pe}, \quad \hat{N}_\theta = (N_\theta)_{pe} \tag{3.9}$$

where $(M_x)_{pe}$, $(M_\theta)_{pe}$, $(N_x)_{pe}$, and $(N_\theta)_{pe}$ given in (3.7) are the respective moments and in-plane forces that are generated by the input of voltage to the patches.

However, if one is using the strong form (2.12) of the equations of motion with piezoceramic actuators, the surface moments and forces to be used in (2.12) are given by

$$\hat{m}_x = -\frac{1}{R}\frac{\partial (M_\theta)_{pe}}{\partial \theta}, \qquad \hat{m}_\theta = -\frac{\partial (M_x)_{pe}}{\partial x}, \tag{3.10}$$

$$\hat{q}_x = -S_{1,2}(x)\hat{S}_{1,2}(\theta)\frac{\partial (N_x)_{pe}}{\partial x}, \qquad \hat{q}_\theta = -S_{1,2}(x)\hat{S}_{1,2}(\theta)\frac{1}{R}\frac{\partial (N_\theta)_{pe}}{\partial \theta}.$$

We point out that the differences between the external surface force expressions in (2.13) and (3.10) are due to the fact that the former were derived for an infinitesimal element whereas the latter are global expressions that preserve the overall signs of the forces generated by the patches as well as reflect the discontinuities due to changes in sign. These differences result from the property that the sense of the forces is highly dependent on the specified location of the axis origin on the neutral surface. Hence the direction of forces throughout the patch differs in some locations from those observed in the infinitesimal element, thus necessitating the inclusion of the indicator functions in (3.10).

Unlike the forces, the action of the moments is specified with respect to a fixed point on the neutral surface (the point 0 for the element in Fig. 2, or a point on the left edge of the shell in Fig. 1). As long as the orientation of the infinitesimal element and full shell with patches are the same, the line moments derived from the infinitesimal element will be consistent with those of the full structure. Thus the expressions for the general infinitesimal moments in (2.13) need no modifications when describing the surface moments generated by the patches as given in (3.10).

4. Patch contributions to plate and beam equations. Analysis similar to that used for the thin cylindrical shells can be used to determine the forces and moments that are due to the presence and activation of piezoceramic patches that have been bonded to a flat plate or beam.

Plate/patch interactions. By repeating the analysis used in the last section for determining the internal moments and forces for the structure consisting of piezoceramic

patches bonded to a thin shell, it is straightforward to show that the internal moments and forces for a *damped* plate having a pair of identical patches with edges at x_1, x_2, y_1, and y_2 are given by

$$N_x = \left[\frac{Eh}{1-\nu^2}(\varepsilon_x + \nu\varepsilon_y) + \frac{c_D h}{1-\nu^2}(\dot{\varepsilon}_x + \nu\dot{\varepsilon}_y)\right] + \left[\frac{2E_1 T}{1-\nu_1^2}(\varepsilon_x + \nu_1\varepsilon_y) + \frac{2c_{D_1} T}{1-\nu_1^2}(\dot{\varepsilon}_x + \nu_1\dot{\varepsilon}_y)\right]\chi_{pe}(x, y),$$

$$N_y = \left[\frac{Eh}{1-\nu^2}(\varepsilon_y + \nu\varepsilon_x) + \frac{c_D h}{1-\nu^2}(\dot{\varepsilon}_y + \nu\dot{\varepsilon}_x)\right] + \left[\frac{2E_1 T}{1-\nu_1^2}(\varepsilon_y + \nu_1\varepsilon_x) + \frac{2c_{D_1} T}{1-\nu_1^2}(\dot{\varepsilon}_y + \nu_1\dot{\varepsilon}_x)\right]\chi_{pe}(x, y)$$

$$N_{xy} = N_{yx} = \left[\frac{Eh}{2(1+\nu)}\varepsilon_{xy} + \frac{c_D h}{2(1+\nu)}\dot{\varepsilon}_{xy}\right] + \left[\frac{E_1 T}{2(1+\nu_1)}\varepsilon_{xy} + \frac{c_{D_1} T}{2(1+\nu_1)}\dot{\varepsilon}_{xy}\right]\chi_{pe}(x, y)$$

and

$$M_x = \left[\frac{Eh^3}{12(1-\nu^2)}(\kappa_x + \nu\kappa_y) + \frac{c_D h^3}{12(1-\nu^2)}(\dot{\kappa}_x + \nu\dot{\kappa}_y)\right] + \left[\frac{2E_1 a_3}{3(1-\nu_1^2)}(\kappa_x + \nu_1\kappa_y) + \frac{2c_{D_1} a_3}{3(1-\nu_1^2)}(\dot{\kappa}_x + \nu_1\dot{\kappa}_y)\right]\chi_{pe}(x, y),$$

$$M_y = \left[\frac{Eh^3}{12(1-\nu^2)}(\kappa_y + \nu\kappa_x) + \frac{c_D h^3}{12(1-\nu^2)}(\dot{\kappa}_y + \nu\dot{\kappa}_x)\right] + \left[\frac{2E_1 a_3}{3(1-\nu_1^2)}(\kappa_y + \nu_1\kappa_x) + \frac{2c_{D_1} a_3}{3(1-\nu_1^2)}(\dot{\kappa}_y + \nu_1\dot{\kappa}_x)\right]\chi_{pe}(x, y),$$

$$M_{xy} = M_{yx} = \left[\frac{Eh^3}{24(1+\nu)}\tau + \frac{c_D h^3}{24(1+\nu)}\dot{\tau}\right] + \left[\frac{E_1 a_3}{3(1+\nu_1)}\tau + \frac{c_{D_1} a_3}{3(1+\nu_1)}\dot{\tau}\right]\chi_{pe}(x, y)$$

(compare to (3.4)). The characteristic function here is given by

$$\chi_{pe}(x, y) = \begin{cases} 1, & x_1 \le x \le x_2,\ y_1 \le y \le y_2, \\ 0, & \text{otherwise}, \end{cases}$$

$a_3 = (h/2 + T)^3 - h^3/8$, and the midsurface characteristics ε_x, ε_y, κ_x, κ_y, ε_{xy}, and τ are defined by

$$\varepsilon_x = \frac{\partial u}{\partial x}, \qquad \varepsilon_y = \frac{\partial v}{\partial y}, \qquad \varepsilon_{xy} = \frac{\partial v}{\partial x} + \frac{\partial u}{\partial y}$$

$$\kappa_x = -\frac{\partial^2 w}{\partial x^2}, \qquad \kappa_y = -\frac{\partial^2 w}{\partial y^2}, \qquad \tau = -2\frac{\partial^2 w}{\partial x \partial y}$$

(see (2.1)). As before, E, c_D, ν and E_1, c_{D_1}, ν_1 are the Young's modulus, damping coefficient, and Poisson ratio for the plate and patches, respectively.

If the patches have differing material properties or if only one patch is present, the moments and forces can be determined from (3.3) with θ replaced by y.

These internal (material) moments and forces are then used in the strong form (2.18) or weak form (2.19) of the plate equations, with the choice depending on the application of interest. In either case, the use of these moments and forces incorporates the structural contributions due to the presence of the piezocermanic patches.

The external moments and forces due to the activation of the patches are also found in a manner analogous to that used in the shell analysis. The induced stresses

$$(\sigma_x)_{pe_1} = (\sigma_\theta)_{pe_1} = -\frac{E_1}{1-\nu_1} e_{pe_1} = -\frac{E_1}{1-\nu_1}\frac{d_{31}}{T} V_1,$$
$$(\sigma_x)_{pe_2} = (\sigma_\theta)_{pe_2} = -\frac{E_2}{1-\nu_2} e_{pe_2} = -\frac{E_2}{1-\nu_2}\frac{d_{31}}{T} V_2$$

are integrated through the thickness of the respective patches, thus yielding the external moments and forces

$$(M_x)_{pe_1} = (M_y)_{pe_1} = -\frac{1}{8}\frac{E_1}{1-\nu_1}\left(4\left(\frac{h}{2}+T\right)^2 - h^2\right) e_{pe_1},$$
$$(M_x)_{pe_2} = (M_y)_{pe_2} = \frac{1}{8}\frac{E_2}{1-\nu_2}\left(4\left(\frac{h}{2}+T\right)^2 - h^2\right) e_{pe_2},$$
$$(N_x)_{pe_1} = (N_y)_{pe_1} = -\frac{E_1 T}{1-\nu_1} e_{pe_1},$$
$$(N_x)_{pe_2} = (N_y)_{pe_2} = -\frac{E_2 T}{1-\nu_2} e_{pe_2}.$$

The total external moments and forces generated by the patches are then given by

$$(M_x)_{pe} = (M_y)_{pe} = [(M_x)_{pe_1} + (M_x)_{pe_2}][H_1(x) - H_2(x)][H_1(y) - H_2(y)],$$
$$(N_x)_{pe} = (N_y)_{pe} = [(N_x)_{pe_1} + (N_x)_{pe_2}][H_1(x) - H_2(x)][H_1(y) - H_2(y)]S_{1,2}(x)\tilde{S}_{1,2}(y), \tag{4.1}$$

where, again, $H_i(x) \equiv H(x - x_i)$, $i = 1, 2$, $S_{1,2}(x)$ denotes the indicator function described in (3.8), and $H_i(y)$ and $\tilde{S}_{1,2}(y)$ are defined in an analogous manner.

These loads can be substituted directly into the weak form of the plate equations (2.19) as the load on the system (with $\hat{q}_n = 0$ and $\hat{N}_x = (N_x)_{pe}$, $\hat{N}_y = (N_y)_{pe}$, $\hat{M}_x = (M_x)_{pe}$, $\hat{M}_y = (M_y)_{pe}$). If the strong form of the plate equations is being used, the surface loads can be determined via the expressions

$$\hat{q}_x = -S_{1,2}(x)\tilde{S}_{1,2}(y)\frac{\partial (N_x)_{pe}}{\partial x}, \qquad \hat{q}_y = -S_{1,2}(x)\tilde{S}_{1,2}(y)\frac{\partial (N_y)_{pe}}{\partial y},$$
$$\hat{m}_x = -\frac{\partial (M_y)_{pe}}{\partial y}, \qquad \hat{m}_y = -\frac{\partial (M_x)_{pe}}{\partial x},$$

and these latter values can be substituted into the equilibrium equations (2.18).

As in the case of the shells, the use of the strong form results in up to two derivatives of the Heaviside function, whereas the use of the weak form alleviates this problem by transferring the derivatives onto the test functions.

It should be noted that the voltage choice $e_{pe} = e_{pe_1} = e_{pe_2}$ causes pure extension (patch pairs excited "in phase") in the plate while pure bending occurs with the choice $e_{pe} = -e_{pe_1} = e_{pe_2}$ ("out of phase" excitation).

Beam/patch interactions. The patch contributions to the dynamics of a thin beam can be determined directly from the plate/patch interaction model if one considers only vibrations in the x direction along with the usual transverse vibrations. For a *damped* beam of thickness h and width b having a pair of bonded patches of thickness T with edges at x_1 and x_2, this yields the internal force and moment

$$
\begin{aligned}
N_x = &\left[Ehb\frac{\partial u}{\partial x} + c_D hb\frac{\partial^2 u}{\partial x \partial t}\right] \\
&+ \left[E_1 b\left(T\frac{\partial u}{\partial x} + \frac{a_2}{2}\frac{\partial^2 w}{\partial x^2}\right) + c_{D_1} b\left(T\frac{\partial^2 u}{\partial x \partial t} + \frac{a_2}{2}\frac{\partial^3 w}{\partial x^2 \partial t}\right)\right]\chi_{pe}(x) \\
&+ \left[E_2 b\left(T\frac{\partial u}{\partial x} - \frac{a_2}{2}\frac{\partial^2 w}{\partial x^2}\right) + c_{D_2} b\left(T\frac{\partial^2 u}{\partial x \partial t} - \frac{a_2}{2}\frac{\partial^3 w}{\partial x^2 \partial t}\right)\right]\chi_{pe}(x) \\
M_x = &\left[E\frac{h^3 b}{12}\frac{\partial^2 w}{\partial x^2} + c_D\frac{h^3 b}{12}\frac{\partial^3 w}{\partial x^2 \partial t}\right] \\
&+ \left[E_1 b\left(\frac{a_2}{2}\frac{\partial u}{\partial x} + \frac{a_3}{3}\frac{\partial^2 w}{\partial x^2}\right) + c_{D_1} b\left(\frac{a_2}{2}\frac{\partial^2 u}{\partial x \partial t} + \frac{a_3}{3}\frac{\partial^3 w}{\partial x^2 \partial t}\right)\right]\chi_{pe}(x) \\
&+ \left[E_2 b\left(-\frac{a_2}{2}\frac{\partial u}{\partial x} + \frac{a_3}{3}\frac{\partial^2 w}{\partial x^2}\right) + c_{D_2} b\left(-\frac{a_2}{2}\frac{\partial^2 u}{\partial x \partial t} + \frac{a_3}{3}\frac{\partial^3 w}{\partial x^2 \partial t}\right)\right]\chi_{pe}(x),
\end{aligned}
\tag{4.2}
$$

where, again, $a_2 = (h/2 + T)^2 - h^2/4$ and $a_3 = (h/2 + T)^3 - h^3/8$. Also, E_1, c_{D_1} and E_2, c_{D_2} denote the Young's modulus and Kelvin-Voigt damping parameter for the individual patches. We note that in obtaining these expressions for the internal forces and moments, we have assumed that the patches also have width b. This was done for clarity of presentation, and more general expressions for the case when the patches are narrower than the beam can be obtained in a similar fashion.

Two special cases of (4.2) are worth mentioning in more detail since they occur quite commonly in applications. If both patches have the same material properties ($E_2 = E_1$ and $c_{D_1} = c_{D_2}$), then (4.2) reduces to

$$
\begin{aligned}
N_x = &\left[Ehb\frac{\partial u}{\partial x} + c_D hb\frac{\partial^2 u}{\partial x \partial t}\right] + \left[2E_1 bT\frac{\partial u}{\partial x} + 2c_{D_1} bT\frac{\partial^2 u}{\partial x \partial t}\right]\chi_{pe}(x) \\
M_x = &\left[E\frac{h^3 b}{12}\frac{\partial^2 w}{\partial x^2} + c_D\frac{h^3 b}{12}\frac{\partial^3 w}{\partial x^2 \partial t}\right] + \left[E_1 b\frac{2a_3}{3}\frac{\partial^2 w}{\partial x^2} + c_{D_1} b\frac{2a_3}{3}\frac{\partial^3 w}{\partial x^2 \partial t}\right]\chi_{pe}(x).
\end{aligned}
$$

If only one patch is present, the expressions reduce to

$$N_x = \left[Ehb\frac{\partial u}{\partial x} + c_D hb\frac{\partial^2 u}{\partial x \partial t}\right] + \left[E_1 b\left(T\frac{\partial u}{\partial x} + \frac{a_2}{2}\frac{\partial^2 w}{\partial x^2}\right) + c_{D_1} b\left(T\frac{\partial^2 u}{\partial x \partial t} + \frac{a_2}{2}\frac{\partial^3 w}{\partial x^2 \partial t}\right)\right]\chi_{pe}(x),$$

$$M_x = \left[\frac{Eh^3 b}{12}\frac{\partial^2 w}{\partial x^2} + \frac{c_D h^3 b}{12}\frac{\partial^3 w}{\partial x^2 \partial t}\right] + \left[E_1 b\left(\frac{a_2}{2}\frac{\partial u}{\partial x} + \frac{a_3}{3}\frac{\partial^2 w}{\partial x^2}\right) + c_{D_1} b\left(\frac{a_2}{2}\frac{\partial^2 u}{\partial x \partial t} + \frac{a_3}{3}\frac{\partial^3 w}{\partial x^2 \partial t}\right)\right]\chi_{pe}(x).$$

When the latter expressions for the internal force and moment resultants are substituted into the strong form (2.21) or weak form (2.22) of the beam equations, it is apparent that the longitudinal and transverse vibrations are coupled as a result of the asymmetry due to the single patch.

The external forces and moments generated by the activation of the patches follow directly from the expressions obtained in the case of the plate. Summarizing from those results, we see that the total external forces and moments are

$$(M_x)_{pe} = [(M_x)_{pe_1} + (M_x)_{pe_2}][H_1(x) - H_2(x)],$$
$$(N_x)_{pe} = [(N_x)_{pe_1} + (N_x)_{pe_2}][H_1(x) - H_2(x)]S_{1,2}(x),$$

where

$$(M_x)_{pe_1} = -\frac{1}{8}E_1 b\left(4\left(\frac{h}{2} + T\right)^2 - h^2\right)e_{pe_1} = -\frac{1}{2}E_1 b(h+T)d_{31}V_1,$$

$$(M_x)_{pe_2} = \frac{1}{8}E_2 b\left(4\left(\frac{h}{2} + T\right)^2 - h^2\right)e_{pe_2} = \frac{1}{2}E_2 b(h+T)d_{31}V_2,$$

$$(N_x)_{pe_1} = -E_1 Tbe_{pe_1} = -E_1 bd_{31}V_1,$$

$$(N_x)_{pe_2} = -E_2 Tbe_{pe_2} = -E_2 bd_{31}V_2.$$

These expressions can then be substituted directly into the weak equations (2.22) as loads on the beam (with $\hat{q}_n = 0$ and $\widehat{N}_x = (N_x)_{pe}$, $\widehat{M}_x = (M_x)_{pe}$). In order to determine the patch loads for the strong form of the beam equations, the corresponding surface moments and forces are found via the relationships

$$(q_x)_{pe} = -S_{1,2}(x)\frac{\partial (N_x)_{pe}}{\partial x}, \qquad (m_y)_{pe} = -\frac{\partial (M_x)_{pe}}{\partial x},$$

and these latter values are used in (2.21). We again point out that this results in the need to differentiate the Heaviside function (once for the force and twice for the moment), whereas this problem is avoided in the weak formulation since the derivatives are transferred on the test functions. In fact, the effect of the Heaviside functions in the latter case is to simply restrict the integrals to the region covered by the patches.

5. Conclusion. In this work, models describing the dynamics of structures consisting of piezoceramic patches which are bonded to an underlying substructure have been presented. While the presentation is for elastic substructures consisting of a thin cylindrical shell, plate, and beam, the techniques discussed for determining the moments and forces generated by the patches can be directly extended to more complex structures and geometries.

In the case of the shell, the patches are assumed to be curved and the coupling between the in-plane strains and the bending, which is due to the curvature, is retained. By bonding the patches to the shell, the material properties of the structure are changed and general expressions for the internal and external moments and forces which incorporate these differences are developed. As demonstrated by the results in [1], it is necessary to account for these differences in material properties in order to match structural frequencies when estimating physical parameters.

A second patch contribution occurs when a voltage is applied and strains are induced. This results in external loads that depend on the material properties of the patches, the geometry of patch placement, and the applied voltages. The expressions for the external moments and forces are sufficiently general so as to allow for differing voltages into the patches, including the possibility of no voltage into a patch (we reiterate that the contributions due to the presence of the passive patch are included in the internal moments).

The techniques for determining the patch contributions to the cylindrical shell equations were then used to develop general models for patches that are bonded to thin flat plates and beams. The importance of careful modeling of the internal moments and forces resulting from the presence of the patches can easily be highlighted in the case of a beam with a single patch bonded to it. Due to the asymmetry of the resulting structure, the resulting internal moments and forces lead to coupling between the PDEs describing the transverse and longitudinal vibrations, which is not accounted for in previous models. As in the shell case, the models are sufficiently general to allow for potentially differing patch voltages, which implies that they can be used for controlling system dynamics when both flexural and extensional vibrations are present.

For each of the shell, plate, and beam interaction models, the contributions of the patches are carefully described in both the strong and weak forms of the time-dependent structural equations of motion. This provides models that can be used in a variety of applications, including numerical simulations, parameter estimation, and control schemes. In each of these applications, the models are sufficiently general to provide for a variety of approximation techniques including modal, spectral, spline, and finite element schemes. Finally, the patch loads determined by these interaction models can be applied to higher-order structural models in exactly the same manner, and analogous models can be used for multiple patch pairs and more complex geometries.

Acknowledgments. The authors would like to express their sincere appreciation to H. C. Lester and R. J. Silcox of the Acoustics Division, NASA Langley Research Center, for many helpful discussions during various phases of this work.

REFERENCES

[1] H. T. Banks, Y. Wang, D. J. Inman, and J. C. Slater, *Variable coefficient distributed parameter system models for structures with piezoceramic actuators and sensors*, Proc. 31st IEEE Conf. Decision and Control, Tucson, AZ, December 16–18, 1992, pp. 1803–1808

[2] R. L. Clark, Jr., C. R. Fuller, and A. Wicks, *Characterization of multiple piezoelectric actuators for structural excitation*, J. Acoustical Soc. Amer. **90**, 346–357 (1991)

[3] E. F. Crawley and E. H. Anderson, *Detailed models of piezoceramic actuation of beams*, AIAA Paper 89-1388-CP, 1989

[4] E. F. Crawley and J. de Luis, *Use of piezoelectric actuators as elements of intelligent structures*, AIAA J. **25**, 1373–1385 (1987)

[5] E. F. Crawley, J. de Luis, N. W. Hagood, and E. H. Anderson, *Development of piezoelectric technology for applications in control of intelligent structures*, Applications in Control of Intelligent Structures, American Controls Conference, Atlanta, June 1988, pp. 1890–1896

[6] E. K. Dimitriadis, C. R. Fuller, and C. A. Rogers, *Piezoelectric actuators for distributed noise and vibration excitation of thin plates*, J. Vibration and Acoustics **13**, 100–107 (1991)

[7] C. L. Dym, *Introduction to the Theory of Shells*, Pergamon Press, New York, 1974

[8] C. R. Fuller, G. P. Gibbs, and R. J. Silcox, *Simultaneous active control of flexural and extensional power flow in beams*, J. Intelligent Materials, Systems and Structures **1**, no. 2, April 1990

[9] C. R. Fuller, S. D. Snyder, C. H. Hansen, and R. J. Silcox, *Active control of interior noise in model aircraft fuselages using piezoceramic actuators*, Paper 90-3922, AIAA 13th Aeroacoustics Conf., Tallahassee, FL, October 1990

[10] G. P. Gibbs and C. R. Fuller, *Excitation of thin beams using asymmetric piezoelectric actuators*, Proc. 121st Meeting ASA, Baltimore, MD, April 1991

[11] N. J. Hoff, *The accuracy of Donnell's equations*, J. Appl. Mech. **22**, 329–334 (1955)

[12] J. Jia and C. A. Rogers, *Formulation of a laminated shell theory incorporating embedded distributed actuators*, The American Society of Mechanical Engineers, Reprinted from *AD-Vol. 15, Adaptive Structures* (B. K. Wada, ed.), Book No. H00533, 1989

[13] S. J. Kim and J. D. Jones, *Optimal design of piezo-actuators for active noise and vibration control*, AIAA 13th Aeroacoustics Conf., Tallahassee, FL, October 1990

[14] H. Kraus, *Thin elastic shells: An introduction to the theoretical foundations and the analysis of their static and dynamic behavior*, John Wiley, New York, 1967

[15] L. D. Landau and E. M. Lifshitz, *Course of Theoretical Physics*, vol. 7: *Theory of Elasticity*, Translated from the Russian by J. B. Sykes and W. H. Reid, Pergamon Press, London, 1959

[16] A. W. Leissa, *Vibration of Shells*, NASA SP-288, 1973

[17] H. C. Lester and S. Lefebvre, *Piezoelectric actuator models for active sound and vibration control of cylinders*, Proc. Conf. Recent Advances in Active Control of Sound and Vibration, Blacksburg, VA, 1991, pp. 3–26

[18] A. E. H. Love, *A Treatise on the Mathematical Theory of Elasticity*, 4th ed., Cambridge Univ. Press, London, 1927

[19] S. Markuš, *The Mechanics of Vibrations of Cylindrical Shells*, Elsevier, New York, 1988

[20] L. S. D. Morley, *An improvement of Donnell's approximation for thin-walled circular cylinders*, Quart. Mech. and Appl. Math. **12**, 89–99 (1959)

[21] A. S. Saada, *Elasticity Theory and Applications*, R. E. Krieger Publ. Co., Malabar, FL, 1987

[22] S. Timoshenko and S. Woinowsky-Krieger, *Theory of Plates and Shells*, 2nd ed., McGraw-Hill, New York, 1987

[23] H. S. Tzou and M. Gadre, *Theoretical analysis of a multi-layered thin shell coupled with piezoelectric actuators for distributed vibration controls*, J. Sound and Vibration **132**, 433–450 (1989)